Energy and Environment Research; Vol. 5, No. 1; 2015
ISSN 1927-0569 E-ISSN 1927-0577
Published by Canadian Center of Science and Education

# The $CO_2$ Gasification Kinetic Study of WEEE Plastic Char Derived from Medium Temperature pyrolysis

Hu Wu[1], Qi An[1], Yafei Shen[1], Noboru Harada[1], Lihao Chen[1] & Kunio Yoshikawa[1]

[1]Department of Environmental Science and Technology, Tokyo Institute of Technology, Yokohama, Japan

Correspondence: Hu Wu, Department of Environmental Science and Technology, Tokyo Institute of Technology, Yokohama, Japan. Tel: 81-45-924-5507. E-mail: wuhu2010wuhu@gmail.com

Received: December 1, 2014 Accepted: December 22, 2014 Online Published: April 12, 2015

doi:10.5539/eer.v5n1p82 URL: http://dx.doi.org/10.5539/eer.v5n1p82

**Abstract**

The isothermal $CO_2$ gasification characteristics of three chars derived from medium temperature pyrolysis of waste electrical and electronic equipment (WEEE) plastics were studied by using a thermogravimetric analyzer (TGA) within the temperature range of 850−1050°C. Phenolic board (PB), brominated high impact polystyrene (HIPS) and acrylonitrile butadiene styrene (ABS) plastics are widely used for the electric and electronic equipment and were employed as model WEEE plastics for the char sample production in this study. The effects of their physicochemical properties and gasification temperature on the WEEE plastic chars conversion rate, the reactivity indexes and the gasification rate were investigated in detail. The random pore model (RPM), the extended random pore model (eRPM) and the shifted extended random pore model (s-eRPM) have been employed to fit the $CO_2$ gasification rate curve of WEEE plastic chars, respectively. The kinetic parameters and the correlation coefficients ($R^2$) were evaluated by RPM, eRPM and s-eRPM, respectively. It was found that the $CO_2$ gasification reactivity of PB char was the highest, followed by that of HIPS char and the gasification reactivity of ABS char was the lowest, which have a close relationship with their pore and carbon crystal structure properties. In addition, it was found that RMP could fit the gasification reaction rate of HIPS char well whose maximum reaction rate appeared at the char conversion of approximate 0.4. Nevertheless, as for PB char and ABS char, their maximum gasification rate presented at char conversion of around 0.8 and 0.2, respectively. And it was observed that eRMP and s-eRPM could predict their gasification rate of PB char and ABS char very well with higher $R^2$, respectively.

**Keywords:** WEEE plastic char, $CO_2$ gasification, kinetics, random pore model, activation energy

## 1. Introduction

Waste electrical and electronic equipment (WEEE) are currently considered to be one of the fastest growing solid waste streams in the world. According to the UNEP report (2009), 40 million tons of WEEE were generated and discharged annually and it was expected an alarming growth per year in the future (United Nations Environment Programme, 2009). For example, in the European Union (EU), more than 9 million tons of WEEE were generated in 2005, and it was expected to grow to more than 12 million tons by 2020 (United Nations Environment Programme, 2009). Additionally, it was well known that there are lots of valuable metals and plastics contained in WEEE, which are worthy recyclable feedstock and could be converted into valuable resources and fuels. On the other hand, WEEE contained certain dangerous and hazardous substances, such as toxic metals and brominated flame retardants, which will pose considerable environmental pollution and health risks if treated inadequately (Yang, Sun, Xiang, Hu & Su, 2013; Ongondo, Williams & Cherrett, 2011). Therefore, how to environmentally soundly and cost-effectively reuse, recycle and recover WEEE has drawn plenty of attention through the world.

Pyrolysis has been proposed as a viable processing route for recycling WEEE, which not only can convert WEEE plastics into fuels and chemical feedstock but also easily separate metals and plastic fractions of WEEE (Yang et al, 2013). However, because of the presence of brominated flame retardants in the WEEE plastics, there are large amount of organic and inorganic brominated compounds existing in the pyrolysis oil, thereby reducing the quality and hindering the reuse of pyrolysis oil. Therefore, lots of debromination methods including the addition of effective catalysts and additives in the pyrolysis process of WEEE plastics have been investigated to reduce the bromine content in the oil products (Yang et al, 2013). Bhaskar et al. synthesized the composite Fe-C

and Ca-C additives, which could effectively remove the brominated compounds from the pyrolysis oil products (Bhaskar et al, 2002; Bhaskar et al, 2003). Terakado and Hirasawa (2011 & 2013) reported that metal oxides used in the pyrolysis of printed circuit boards containing brominated flame retardants could effectively suppress the formation of HBr and brominated organic compounds. Besides, there were many researches on zeolite catalysts used for the debromination in the pyrolysis of brominated WEEE plastics (Hall & Williams, 2008; Bozi & Blazsó, 2009; Hall, Miskolczi, Onwudili & Williams, 2008). The above research results indicated that the pyrolysis process could effectively convert the WEEE plastic into valuable, storable and transportable oil products used for fuel and chemical feedstock. In addition, they showed that metal recovery from the pyrolysis residues was relatively easy due to their friable and loose structure property (Zhang, Yoshikawa, Nakagome & Kamo, 2013).

However, after the low-medium temperature pyrolysis process, about 20 wt.% of WEEE plastic char remained (Hall & Williams, 2008), which is worth recyclable resource in order to increase the recycle efficiency of WEEE plastics. On the other hand, the existence of the char would be a potential problem for the recycling of further metal screening and refinement. The gasification behaviors of coal char and biomass char have already been widely studied (Zhang, Ashizawa, Kajitani & Miura, 2008; Zhang, Hara, Kajitani & Ashizawa, 2010; Yuan, Chen, Li & Wang, 2011; Jing et al, 2013). For instance, Zhang et al. (2008) have investigated the steam gasification of 14 kinds of biomass chars and found that the extended random pore model could predict the gasification rates of all 14 kinds of biomass chars very well. Jing et al. (2013) studied the $CO_2$ gasification behaviors of various coal chars and concluded that the $CO_2$ gasification behaviors had a close relationship with their physicochemical Properties, especially with the $CO_2$ chemisorbed volumes of chars. With regard to biomass and coal chars, the intrinsic alkali (K and Na), alkaline (Ca and Mg) and transition (Fe) metal contents also play important roles on the char gasification rates (Zhang, et al. 2008; Yuan et al., 2011; Lahijania, Zainala, & Mohamedb, 2012). In addition, the Si and Al metal contents generally exert severe inhibition effect on the gasification reaction (Zhang, et al., 2008; Zhang, et al., 2010; Yuan, et al., 2011). Consequently, for different biomass and coals char containing various amount of alkali and alkaline metal contents, their gasification performance are totally different. However, there are few alkali and alkaline metals exist in the WEEE plastic chars and few attempts have been made to investigate the $CO_2$ gasification reactivity of WEEE plastic chars derived from the medium-temperature pyrolysis (Gil, Fermoso, Pevida, Pis & Rubiera 2010). Additionally, the $CO_2$ gasification reactivity of chars is lower than that of $O_2$ or $H_2O$ gasification, and consequently, it is regarded as the rate-determining step in the gasification process (Jing et al, 2013). The $CO_2$ gasification of WEEE plastic char might prevent the oxidation of metals existing in the chars. To this end, it is of great significance to understand the $CO_2$ gasification behavior of WEEE plastic char. The gasification reactivity and kinetic parameters are essential for the efficient and reliable design of the gasification system. Thermogravimetric analysis (TGA) is an ideal instrument for investigating the gasification characteristics of carbonaceous materials because of its high accuracy, simplicity of design and ease of operation (Yuan et al, 2011). By means of TGA, different models can be applied to evaluate the kinetic parameters and the activation energy.

In this study, the isothermal $CO_2$ gasification behaviors of three WEEE plastics (PB, HIPS and ABS) chars derived from the pyrolysis at 600°C were investigated by using the thermogravimetric analysis (TGA) at the temperatures of 850-1050 °C. Effects of the plastic char types, the reaction temperature on the char conversion, the reactivity index and the gasification rate were investigated in detail. Moreover, RPM, eRPM and s-eRPM were employed to fit the gasification rate of three WEEE plastic char at different temperatures in order to determine their gasification correlation coefficients, kinetic parameters and activation energies, respectively.

## 2. Experimental

### *2.1 Preparation of Samples*

Three char samples were collected from our previous pyrolysis experiments of three typical WEEE plastics, i.e. phenolic board (PB), brominated high impact polystyrene (HIPS) and acrylonitrile butadiene styrene (ABS), respectively. In brief, 30g of each WEEE plastic was pyrolyzed in a quartz fixed-bed reactor, which was heated to 600 °C at a heating rate of 100 °C/min. The flow rate of the carrier gas ($N_2$) was 50 mL/min. After the reactor temperature reached 600 °C, it was held at this temperature for 2 hours and was then cooled quickly. Subsequently, three chars were collected, ground and sieved to obtain the powder char sample with a size between 150 and 250 μm. Three char samples were denoted by PB char, HIPS char and ABS char, respectively. The proximate and ultimate analysis were conducted according to ASTM D7582 and ASTM D3176 by DTG-50 TGA and JM 10 elemental analyzer, respectively. And the ash compositions of char samples were analyzed by the XRF. The analysis results are shown in Table 1.

Table 1. The proximate analysis, ultimate analysis and ash analysis of char samples

| Sample | PB | HIPS | ABS |
|---|---|---|---|
| *Proximate analysis (wt.%)* | | | |
| Moisture | 0.4 | 1.4 | 1.4 |
| Volatile matter | 21.5 | 19.1 | 15.5 |
| Fixed carbon | 76.8 | 53.1 | 73.8 |
| Ash | 1.3 | 26.5 | 9.3 |
| *Ultimate analysis (wt.%)* | | | |
| C | 90.7 | 94.6 | 95.3 |
| H | 2.2 | 2.8 | 1.4 |
| N | 0.3 | 0.3 | 1.7 |
| Br | 0.0 | 2.2 | 1.6 |
| O[a] | 6.8 | 0.0 | 0.0 |
| *Ash content (wt.% in ash)* | | | |
| Sb | 0.0 | 2.8 | 60.1 |
| Ti | 0.0 | 73.1 | 0.5 |
| Fe | 18.1 | 4.2 | 10.6 |
| Cr | 17.4 | 0.9 | 3.4 |
| Ca | 0.0 | 2.6 | 4.6 |
| Cu | 20.7 | 0.0 | 0.0 |
| Br | 0.0 | 13.4 | 12.0 |

[a] By difference

*2.2 Analytical Methods*

The CHN element analysis was conducted by using a Micro Corder JM 10 Elemental Analyzer. The bromine contents of the char was determined by using an air combustor coupled with Dionex ICS-1100 ion chromatography fitted with a **Shodex** IC**S1-904E** column according to JIS K 7392. The ash compositions of the char were determined by an energy dispersive X-ray fluorescence spectrometer (XRF) under vacuum mode for precise measurement. A powder X-ray diffraction (XRD) analysis was carried out for the verification of the crystallinity of three chars. XRD measurements were performed using a Rigaku Ultimal V diffractometer with the CuKα radiation (λ = 1.540) at 40kV and 40 mA. The XRD patterns were accumulated in the range of 5–50° every 0.02° (2θ) with the counting time of 1 s per step. The surface structure property was analyzed by the SEM. Surface area and textural properties of the used catalysts were determined by $N_2$ physical adsorption at 77 K, applying the Brunauer–Emmett–Teller (BET) method, using a Micromeritics Tristar 3020 equipment.

2.3 Experimental procedure and reactivity measurements

The isothermal $CO_2$ gasification experiments were conducted using the Shimadzu DTG-50 thermogravimetric analyzer. 10 mg of char sample was filled into a cylindrical alumina crucible and then was heated to the targeted temperature at the heating rate of 30 °C/min under $N_2$ atmosphere with a flow rate of 150 mL/min. After that, the temperature was kept at the targeted temperature for 10 minutes to maintain the thermal and weight equilibrium. Subsequently, the carrier gas was switched to $CO_2$ with the same flow rate to carry out the isothermal $CO_2$ gasification until the char sample weight became constant. The time when $CO_2$ was injected was defined as t = 0. The carbon conversion (X) and the gasification rate (r) of chars in the gasification experiment were calculated by the following equation:

$$X = \frac{W_0 - W_t}{W_0 - W_a} \quad (1)$$

$$\mathrm{r} = \frac{\mathrm{d}X}{\mathrm{d}t} \quad (2)$$

Where $W_0$ (mg) is the initial char weight at the gasification time $t = 0$. $W_t$ (mg) is the instantaneous sample weight at the gasification time of $t$, and $W_a$ (mg) is the left ash weight after finishing gasification. The reactivity index Rs has been widely used to compare the gasification reaction reactivity between different samples. It is given by $Rs = 0.5/t_{0.5}$ with $t_{0.5}$ being the time required for 50% carbon conversion (Lahijani Zainal, Mohamed & Mohammadi, 2013).

*2.4 Kinetic Models*

The most widely used oxygen-exchange mechanism for the $CO_2$ gasification of char, proposed by Reif (Reif, 1952), can be summarized as

$$C_f + CO_2 \leftrightarrow C(O) + CO \quad (3)$$

$$C(O) \rightarrow CO + C_f \quad (4)$$

Where $C_f$ denotes a free carbon active site and C(O) denotes a carbon-oxygen complex.

According to above mechanism, various kinetic models have been proposed and investigated to characterize the $CO_2$ gasification of char, such as the homogeneous model, the shrinking model, the random pore model and the extended random pore model and the shifted extended random pore. In this work, three typical kinetic models, the random pore model (RPM), the extended random pore model (eRPM) and the shifted extend random pore model (s-eRPM) were used to characterize the $CO_2$ gasification of char in the absence and presence of carbonate catalysts. RPM, proposed by Bhatia and Perlmutter (1980), was developed on the base of overlapping cylindrical pores mechanism, which means that there are arbitrary pore size distributions in the char particle and all pores grow and coalesce as the reaction progresses. The reaction rate is expressed as:

$$\frac{dX}{dt} = K(1-X)\sqrt{1-\Psi \ln(1-X)} \quad (5)$$

$$K = k_0 P_{CO_2}^n \exp\left(-\frac{E_a}{RT}\right) \quad (6)$$

Where X is the char conversion, K is the rate constant for the reaction on the pore surfaces, Ψ is the pore surface parameter, $k_0$ ($min^{-1}$) is the pre-exponential factor, Ea (kJ/mol) is the activation energy, and $P_{CO2}$ (bar) is the $CO_2$ partial pressure. And the parameter Ψ can be calculated by the following equation:

$$\Psi = \frac{4\pi L_0(1-\varepsilon_0)}{S_0^2} \quad (7)$$

Where $S_0$, $L_0$ and $\varepsilon_0$ denote the pore surface area, the pore length and the total volume of the solid porosity, respectively.

RPM have been successfully used for modeling the gasification reaction of chars. However, it failed to describe the reactivity profiles of biomass chars or alkali metals catalyzed char, for which the reactivity increases with the increase of the conversion or exists a maximum gasification rate in higher or lower char conversion range (Zhang et al, 2008; Zhang et al, 2010). Therefore, the eRPM was proposed by Zhang et al (2008) by introducing empirical parameters c and p to better fit the experimental data obtained from the alkali metal catalyzed gasification of coal char and biomass char. The eRPM is expressed in the equation (9).

$$\frac{dX}{dt} = K(1-X)\sqrt{1-\varphi \ln(1-X)}\,(1+(cX)^p) \quad (8)$$

Where c is a dimensionless constant, and p is a dimensionless power law constant. If c = 0, eRPM becomes the same as RPM. However, it was reported that when the maximum gasification rate appears in the lower char conversion interval, the eRPM also cannot perform well (Yuan et al, 2011; Jing et al, 2013). The shifted extended random pore model (s-eRPM) was proposed by changing the conversion term $(1 + (cX)^p)$ of eRPM from multiplication to division in order to fit the gasification rate when maximum rate appears at lower char conversion (< 0.2) (Jing et al, 2013). The s-eRPM could be written by the following equation.

$$\frac{dX}{dt} = \frac{K(1-X)\sqrt{1-\varphi \ln(1-X)}}{1+(cX)^p} \quad (9)$$

In this study, the rate constant K, the structure parameter Ψ and two semi-empirical parameters c and p are independent of the temperature and estimated by the nonlinear least-squares method in the MATLAB software.

## 3. Results and Discussions

*3.1. Characteristics of Char Samples*

From the proximate and ultimate analysis shown in Table 1, it is found that the three chars derived from the pyrolysis at 600 $^oC$ still contained certain amount of volatile matter and various amount of ash and fixed carbon. For instance, the weight percent of fixed carbon in the PB char, HIPS char and ABS char is 76.8 wt.%, 53.1 wt.% and 73.8 wt.%, respectively. And the ash content of HIPS char is the highest (26.5 wt.%) while the ash content of

PB char is the lowest (1.3 wt.%). The main compositions of HIPS char ash are Ti and Br elements. And the major components of the ABS char was the Sb and Br. The metal element, such as Ti and Sb, come from the synergist additives and the Br element mainly derived from the brominated flame retardant. The synergist additive and brominated flame retardant are often fed into the WEEE plastic in an attempt to reduce its flammability (Yang et al, 2013; Hall et al, 2008). Additionally, there are some Fe element exist in the ash fractions for three chars, which might come from the steel reactor when the WEEE plastics were pyrolyzed.

The surface morphology characteristics of chars could be a very important parameter to evaluate the $CO_2$ gasification reactivity of char, which were observed by using SEM and are shown in Figure 1. The morphological structure of PB char showed irregular and sharp-edged property. The PB char exhibited porous and textural structure characteristics, which was in accordance with previous researches (Ke, Yang, Liu, Liu & Dong, 2013). As for the HIPS char, it was observed that HIPS char consisted of small relatively uniform particles and each particle are smooth and compressed. There were some porosity structure during each particle. A significant difference in morphology can be seen for the ABS char. The surface of ABS char was smooth and compact. No obvious pore structure was found in the surface of ABS char, which might be attributed to the agglomeration and melting during the pyrolysis of ABS plastic.

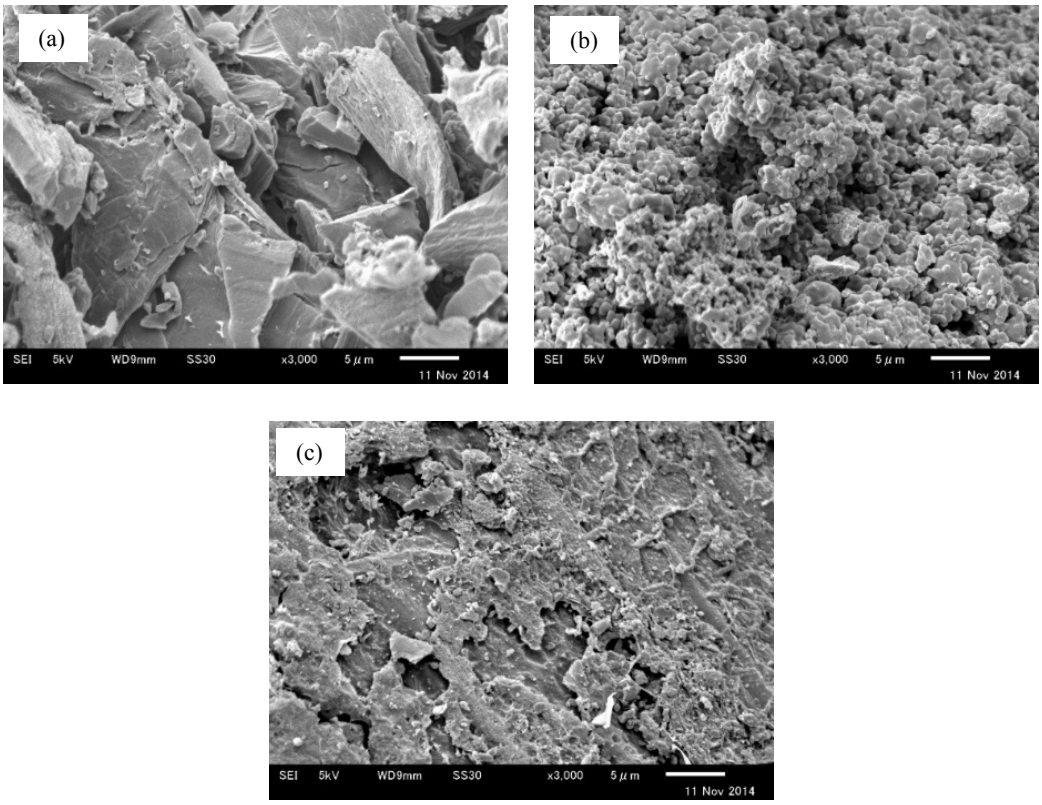


Figure 1. SEM micrographs (3,000X) of WEEE plastic chars: (a) PB Char, (b) HIPS Char, (C) ABS Char

Table 2. The pore structure properties of WEEE plastic chars

| Char Samples | BET surface area ($m^2/g$) | Micropore volume ($cm^3/g$) | Average pore diameter (nm) |
|---|---|---|---|
| PB Char | 309.32 | 0.136 | 4.47 |
| HIPS Char | 105.91 | 0.073 | 8.09 |
| ABS Char | 30.16 | 0.04 | 12.36 |

The pore structure characteristics of WEEE plastic chars were analyzed by $N_2$ adsorption-desorption whose results are shown in Table 2. It indicated that the PB char was more porous than the other two chars. For example, PB char has the largest BET surface area and micropore volume (309 $m^2/g$ and 0.136 $cm^3/g$, respectively), which are much larger than those of ABS char (30.16 $m^2/g$ and 0.04 $cm^3/g$, respectively). With regard to the surface

area, it was considered to play a vital role in determining the gasification reactivity, which was attributed to the fact that the surface area could provide active sites and the char gasification reactivity was proportional to active sites and active surface area. For the pore size, it was reported that only the pores with diameters larger than 1.5 nm can contribute to the $CO_2$ gasification reaction (Yuan et al, 2011). Furthermore, the pore size distribution would influence the diffusion of reactants and products (Jing et al, 2013). As shown in Table 2, it was found that the average pore diameter of PB char was much smaller than those of HIPS char and ABS char, which indicated that PB char are richer in micro- and mesopores than those of HIPS char and ABS char. Therefore, the gasification reactivity of PB char is expected to be more active than those of HIPS char and ABS char.

The carbon crystalline structure is another essential feature of char, which is closely associated with the char $CO_2$ gasification behavior. Liu and co-workers reported that the carbon crystalline structure exerted greater effect on the gasification reactivity than the porosity structure for the chars prepared at different pyrolysis conditions (Jing et al, 2013; Huang, et al, 2009). In the studies by Jing et al. (2013), the carbon crystalline structure performed better than the alkali index and BET surface area on the correlation with the gasification reactivity for the different coal chars. According to the XRD patterns in Figure 2, the crystal plane index C(002) peaks were observed at approximately 24° in the all XRD spectrums of WEEE plastic chars. The C(002) diffraction peak represents the degree of parallel and azimuthal orientation of the aromatic lamellae (Huang, et al, 2009). The disordering of carbon crystalline structure results in the broadening of the C(002) diffraction peak: the more disordering of carbon crystalline structure, the wider the diffraction peak of C(002). It was found that the C(002) diffraction peak of ABS char was narrow and sharp while the C(002) peak of PB char was flat and wide. The width and height of HIPS char were between those of PB char and ABS char. It indicated that the carbon crystalline degree in the three chars was in the sequence of ABS char > HIPS char > PB char. Therefore, it was predicted that the gasification reactivity of three was in the order of PB char > HIPS char > ABS char. Additionally, as for HIPS char, the sharp peaks at around 27.6°, 36.5° and 41.9° represent $TiO_2$, while in the case of ABS char, the peaks at 28.9°, 32.2° and 44.5° are related to the presence of $Sb_2O_3$. As mentioned above, the $TiO_2$ and $Sb_2O_3$ are commonly employed as synergist and added in WEEE plastic to reduce its flammability (Yang et al, 2013; Hall et al, 2008).

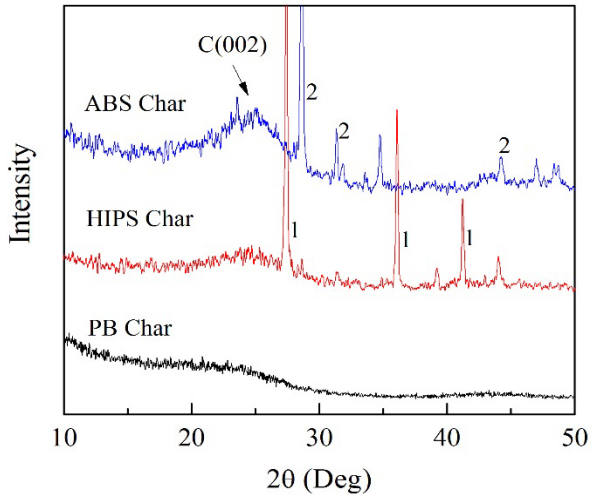


Figure 2. XRD patterns of WEEE plastic chars (1, $TiO_2$; 2, $Sb_2O_3$)

According to the analytical results discussed above, the conclusion could be drawn that the characteristics of three WEEE plastic chars are significantly different in the terms of the surface area, pore structure and the carbon crystalline structure. The effect of these properties on the gasification reactivity will be investigated in detail in the following section.

*3.2 Effect of the Gasification Temperature on the Char Conversion*

It is well known that the gasification temperature is an essential parameter in controlling the gasification reactivity of char. Therefore, the isothermal $CO_2$ gasification of PB char, HIPS char and ABS char was firstly conducted in the range of 850 – 1050 $^oC$, and the result is shown in Figure 3. It indicated that, for all char samples, with the increase of the gasification temperature, the time for the total carbon conversion decreased. For instance, in the case of HIPS char, the gasification time required for the total carbon conversion was over 200 minutes at 850 $^oC$, while the gasification time decreased to 27 minutes at 1050 $^oC$. The gasification of HIPS at

1050 °C was approximately 7.3 times faster than that at 850 °C. As for PB char, the gasification time at 1050 °C was 11.7 times shorter than that at 850 °C. Meanwhile, in the case of ABS char, the gasification time at 850 °C was 3.8 times longer than that at 1050 °C. It illustrated that the higher the gasification temperature is, the faster the char conversion becomes for all samples. Additionally, it indicated that the gasification behavior of the three samples were significantly different because of their various physicochemical properties. At the gasification temperature of 850 °C, the time for the total char conversion of PB char, HIPS char and ABS char were 175.1, 204.7 and 238.2 minutes, respectively, while when the gasification was 1050 °C, the time for the total char conversion of PB char, HIPS char and ABS char were 15.2, 28.1 and 63.6 minutes, respectively. It was found that under the same gasification temperatures, the gasification reactivity of PB char was found to be the highest, followed by that of HIPS char, and the gasification reactivity of ABS char was the lowest, which might be attributed to its smallest surface area and most compact pore structure property, as shown in Figure 2 and Table 2.

In order to compare the gasification reactivity of three WEEE plastic chars in detail, the reactivity index Rs, proposed by Takarada et al. (1985), have been calculated in the temperature range of 850 °C – 1050 °C. It is given by $Rs = 0.5/t_{0.5}$ with $t_{0.5}$ being the time required for 50% conversion of the fixed carbon. The results are listed in Table 3, which illustrates that the reactivity index is in good agreement with the above mentioned result that the reactivity index of PB char was the highest, followed by that of HIPS and the reactivity index of HIPS was the lowest for all of the temperatures. In addition, as the increase of the gasification temperature, the reactivity index for each char also improved significantly.

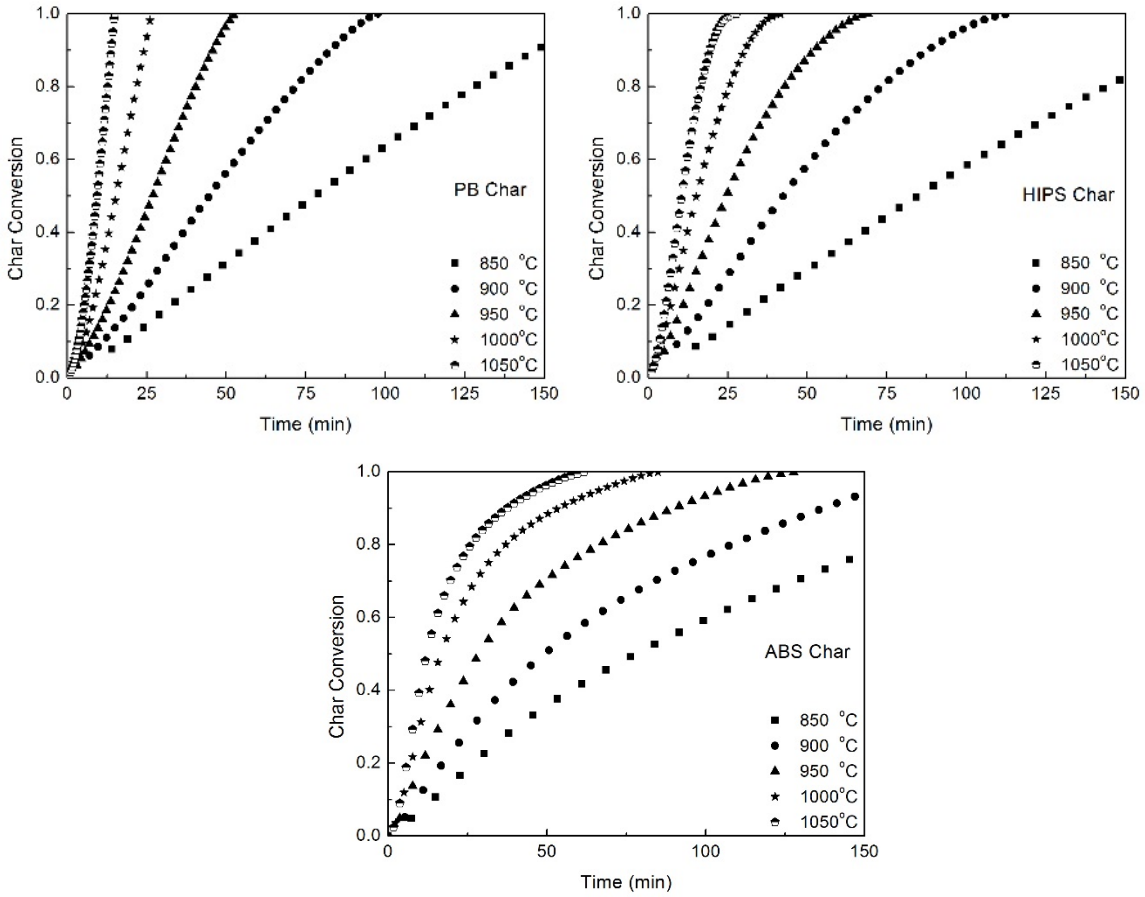


Figure 3. The effect of the gasification temperature on the PB, HIPS and ABS char conversion curves

Table 3. The $CO_2$ gasification reactivity indexes of PB char, HIPS char and ABS char at different temperatures

| Rs | 850 °C | 900 °C | 950 °C | 1000 °C | 1050 °C |
|---|---|---|---|---|---|
| PB Char | 0.00640 | 0.01171 | 0.02165 | 0.03373 | 0.05360 |
| HIPS Char | 0.00589 | 0.01157 | 0.02045 | 0.03216 | 0.04770 |
| ABS Char | 0.00569 | 0.01016 | 0.01745 | 0.03014 | 0.04115 |

### *3.3. Kinetic Analyses of $CO_2$ Gasification of WEEE Plastic Chars*

The effect of the temperature on the gasification reaction rate was investigated in the temperature range of 850 $^oC$ – 1050 $^oC$, whose result is shown in Figure 4. It is worth mentioning that all of the gasification rates firstly increase to the maximum and then gradually decline with the char conversion. It was reported that this behavior may be attributed to char structure evolution during the reaction process. It is that in the initial stage, the porosity is lower and the original blocked pores are opened and grow, which can improve the surface area available for the reaction. Subsequently, the overlapping of pore structure occurs originating to collapse of the macropore and coalescence of the neighboring pores as gasification proceeds, which would lead to the reduction of the surface area available for the reaction (Ochoa, Cassanello, Bonelli & Cukierman, 2001; Zhang et al, 2008). However, with regard to the different chars, the maximum gasification rate appeared in different carbon conversion ranges. As for the PB char, the maximum gasification rate appeared at the char conversion of approximate 0.8. In the case of HIPS char and ABS char, the maximum gasification rate was obtained when the carbon conversion was about 0.45 and 0.2, respectively. In addition, as expected, the reaction rate results were consistent with that of char conversion, which was sensitive to the gasification temperature and the reactivity was improved as the temperature increased. The experimentally obtained gasification rate results would be used for the kinetic study.

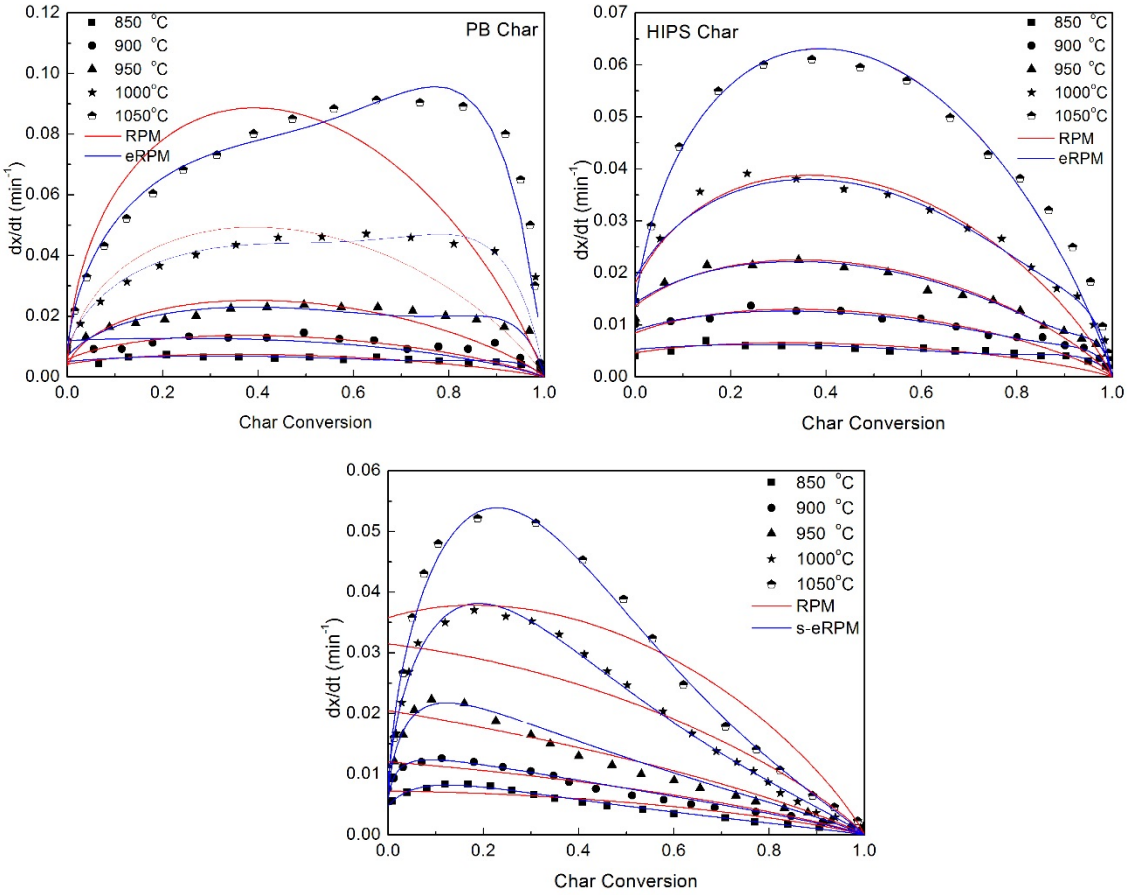


Figure 4. Gasification rates of PB char, HIPS char and ABS char (symbols) and fitting curves of RPM, eRPM and s-eRPM (lines)

Several kinetic models have been applied to simulate the gasification reactions and describe the relationship between the reaction rate and time, such as the homogeneous model, the shrinking core model, the normal distribution model, RPM, eRPM and s-eRPM. It could be obviously found that there was a maximum for the gasification rate of each char as shown in Figure 4. In the above mentioned models, only RPM and eRPM are suitable to simulate this gasification behavior (Zhang et al, 2008; Jing et al, 2013). The equations and the meanings of each parameters of RPM and eRPM have been shown and explained in the session 2.4. The reaction rate of three chars at different temperatures have been simulated by both RPM and eRPM, respectively. The MATLAB software was employed to fit the experimental reaction rate results by the nonlinear least-squares

methods in order to estimate the kinetic parameters and the correlation coefficients ($R^2$). And the curve fitting results and the estimated kinetic parameters results are presented in Figure 4 and Table 4, respectively. From the curve fitting results, as for PB whose maximum gasification rate appeared at the char conversion of about 0.8, eRPM was better than RPM to predict the gasification rate. The maximum gasification rate of HIPS char was obtained at the char conversion of about 0.4. The curve fitting result of RPM and eRPM for the HIPS char gasification rate were almost comparable. Nevertheless, for ABS char, the RPM and eRPM could not simulate the gasification rate very well, because the maximum gasification rate of ABS char appeared at the char conversion of less than 0.2 because of the smallest surface area (Jing et al, 2013). It was reported that when the maximum gasification rate appeared at a lower char conversion, the s-eRPM, as shown in equation 9, was more suitable for the gasification rate curve fitting (Yuan et al, 2011; Jing et al, 2013). It was found that the s-eRPM could fit the gasification rate curve of ABS well with a higher $R^2$ valve over 0.99. The Jing and co-worker (2013) reported that the better curve fitting results of eRPM and shifted eRPM than that of RPM illustrated that the gasification of coal char is not only affected by the initial pore structure but also the inherent minerals and variation of the pore structure in the gasification process.

Furthermore, Table 4 indicates that the value of Ψ increased as the temperature was raised from 850 $^{o}$C to 1050 $^{o}$C, which demonstrates that char porosity development and the progress of reactions occurred inside the pores of chars with the increase of the temperature, which was one of reasons why at a higher temperature, the gasification reactivity was higher.

Table 4. The kinetic parameters and regression coefficients estimated by the RPM and eRPM fitting

| Sample | T | Kinetic Parameters | | | | | | | |
|---|---|---|---|---|---|---|---|---|---|
| | | RPM | | | e-RPM/s-eRPM[a] | | | | |
| | ℃ | K | ψ | $R^2$ | K | ψ | c | p | $R^2$ |
| PB Char | 850 | 0.0042 | 14.7 | 0.931 | 0.005 | 7.67 | 1.2 | 9.85 | 0.993 |
| | 900 | 0.0057 | 29.0 | 0.972 | 0.012 | 1.70 | 0.6 | 0.95 | 0.994 |
| | 950 | 0.0035 | 286.9 | 0.951 | 0.007 | 62.18 | 1.2 | 8.89 | 0.991 |
| | 1000 | 0.0048 | 574.9 | 0.945 | 0.009 | 131.73 | 1.2 | 5.63 | 0.992 |
| | 1050 | 0.0035 | 572.1 | 0.944 | 0.009 | 384.52 | 1.3 | 4.45 | 0.994 |
| HIPS Char | 850 | 0.0046 | 8.8 | 0.989 | 0.005 | 5.00 | 1.1 | 10.47 | 0.993 |
| | 900 | 0.0084 | 10.8 | 0.991 | 0.009 | 8.49 | 1.1 | 15.71 | 0.994 |
| | 950 | 0.0137 | 12.6 | 0.987 | 0.014 | 11.15 | 1.0 | 25.50 | 0.998 |
| | 1000 | 0.0180 | 23.1 | 0.990 | 0.019 | 19.48 | 1.0 | 15.98 | 0.995 |
| | 1050 | 0.0139 | 110.2 | 0.987 | 0.014 | 110.20 | 1.0 | 117.42 | 0.996 |
| ABS Char | 850 | 0.0072 | 1.7 | 0.871 | 0.005 | 48.4 | 3.5 | 1.17 | 0.991 |
| | 900 | 0.0121 | 1.9 | 0.866 | 0.006 | 196.1 | 17.1 | 0.71 | 0.992 |
| | 950 | 0.0204 | 2.7 | 0.894 | 0.007 | 213.4 | 4.7 | 1.05 | 0.995 |
| | 1000 | 0.0315 | 3.4 | 0.887 | 0.0093 | 276.2 | 2.16 | 1.71 | 0.996 |
| | 1050 | 0.0358 | 4.4 | 0.853 | 0.0078 | 395.0 | 1.78 | 2.18 | 0.997 |

[a] For PB char and HIPS char, eRPM is used; For ABS char, s-eRPM is employed.

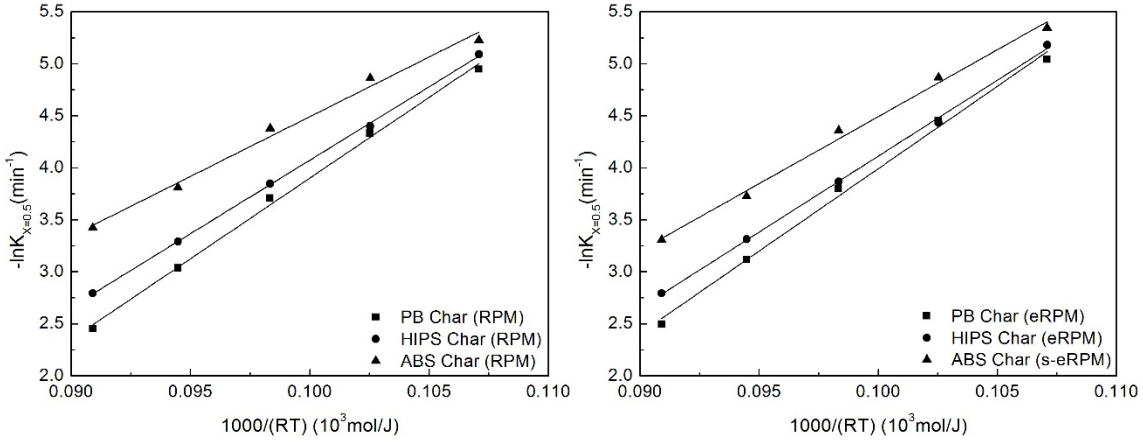


Figure 5. Arrhenius curves of WEEE plastic chars gasification reaction by employing RPM, eRPM and s-eRPM

Table 5. Activation energy $E_a$ and the pre-exponentional factor $k_0$ calculated by Arrhenius equation

| | RPM | | eRPM/s-eRPM | |
|---|---|---|---|---|
| Sample | $E_a$ (kJ/mol) | $k_0$ (min$^{-1}$) | $E_a$ (kJ/mol) | $k_0$ (min$^{-1}$) |
| PB Char | 155.11 | $1.10\times10^5$ | 158.44 | $1.40\times10^5$ |
| HIPS Char | 141.18 | $2.30\times10^4$ | 145.94 | $3.56\times10^4$ |
| ABS Char | 114.77 | $1.08\times10^3$ | 128.70 | $4.34\times10^3$ |

It have been mentioned that the rate constant K in the above discussed models would become the initial gasification rate d$X$/d$t$ when char conversion X = 0. Nevertheless, it was reported that the switch of gas results for $dX/dt$ (X = 0) obtained from the TGA is not accurate (Kajitani, Hara & Matsuda, 2002; Yuan et al, 2011; Jing et al, 2013). Consequently, in this study, the gasification rate at char conversion of 0.5 ($r_{0.5}$) was taken as the basis and the $lnr_{0.5}$ versus $1/(R\cdot T)$ is plotted in Figure 5. According to the RPM, eRPM and s-eRPM, the activation energy $E_a$ and the pre-exponentional factor $k_0$ could be calculated by the Arrhenius equation, and the results are shown in Table 5. It can be observed that the values of activation energies of three chars obtained from eRPM and s-eRPM are a little higher than that of three chars obtained from RPM. According the best fitting model, the activation energies of PB char, HIPS char and ABS char are 158.44, 145.94 and 128.70 kJ/mol, respectively.

## 4. Conclusion

The $CO_2$ gasification of PB char, HIPS char and ABS char were conducted at the temperature range of 850-1050 $^oC$ in the TGA. The main conclusions from this work are summarized as follows: (1) As expected, for all three char samples, with the increase of the gasification temperature, the time for the char conversion decreased while the reactivity index and the gasification rate significantly increased. The reactivity indexes of PB char, HIPS char and ABS char at 1050 $^oC$ became 8.4, 8.1 and 7.2 times higher than that of them at 850 $^oC$, respectively. (2) At the same gasification temperature, the gasification reactivity of three WEEE plastic chars was in the order of PB char > HIPS char > ABS char, which was attributed to the fact that the surface area of PB char is the largest and lowest carbon crystalline degree. (3) For PB char, its maximum gasification rate appears in the char conversion of approximate 0.8 and the best fitting curve model was eRPM with the highest $R^2$ (> 0.991). As for HIPS char, RPM and eRPM are comparably suitable to fit the gasification rate curve, and $R^2$ of RPM and eRPM are > 0.985 and > 0.993, respectively. In the case of ABS char, the maximum gasification rate presents in the lower carbon conversion (< 0.2), and s-eRPM was the most suitable model for predicting the gasification rate with the highest $R^2$ (> 0.991). (4) The $CO_2$ gasification activation energies of PB char, HIPS char and ABS char are 158.44, 145.94 and 128.70 kJ/mol, respectively.

## References

Bhaskar, T., Matsui, T., Uddin, M. A., Kaneko, J., Muto, A., & Sakata, Y. (2003). Effect of Sb2O3 in brominated

heating impact polystyrene (HIPS-Br) on thermal degradation and debromination by iron oxide carbon composite catalyst (Fe-C). *Applied Catalysis B: Environmental, 43*, 229–241. http://dx.doi.10.1016/S0926-3373(02)00306-5

Bhaskar, T., Matsui, T., Kaneko, J., Uddin, M. A., Muto, A., & Sakata, Y. (2002). Novel calcium based sorbent (Ca-C) for the dehalogenation (Br, Cl) process during halogenated mixed plastic (PP/PE/PS/PVC and HIPS-Br) pyrolysis. *Green Chemistry, 4*, 372–375. http://dx.doi.10.1039/b203745a

Bhatia, S., & Perlmutter, D. (1980). A random pore model for fluid-solid reactions: I. Isothermal, kinetic control. *AIChE J, 26*(3), 379−386. http://dx.doi.org/10.1002/aic.690260308

Bozi, J., & Blazsó, M. (2009). Catalytic modification of pyrolysis products of nitrogen-containing polymers over Y zeolites. *Green Chemistry, 11*, 1638–1645. http://dx.doi.10.1039/b913894n

Gil, M. V., Fermoso, J., Pevida, C., Pis, J. J., & Rubiera, F. (2010). Intrinsic char reactivity of plastic waste (PET) during $CO_2$ gasification. *Fuel Processing Technology, 91*, 1776–1781. http://dx.doi.org/10.1016/j.fuproc.2010.07.019

Hall, W., & Williams, P. T. (2008). Removal of organobromine compounds from the pyrolysis oils of flame retarded plastics using zeolite catalysts. *Journal of Analytical and Applied Pyrolysis, 81*, 139-147. http://dx.doi.10.1016/j.jaap.2007.09.008

Hall, W. J., Miskolczi, N., Onwudili, J., & Williams, P. T. (2008). Thermal Processing of Toxic Flame-Retarded Polymers Using a Waste Fluidized Catalytic Cracker (FCC) Catalyst. Energy & Fuels, 22, 1691–1697. http://dx.doi.10.1021/ef800043g

Huang, Y., Q., Yin, X., L, Wu, C., Z., Wang, C., W., Xie, J., J., Zhou, Z., Q., Ma, L., L. & Li, H., B. (2009). Effects of metal catalysts on $CO_2$ gasification reactivity of biomass char. *Bitechnology Advances, 27*, 568-572. http://dx.doi.org/10.1016/j.biotechadv.2009.04.013

Jing, X. L., Wang, X. Q., Zhang, Q., Yu, Z. L., Li, C. Y., Huang, J. J., & Fang, Y. (2013). Evaluation of $CO_2$ Gasification Reactivity of Different Coal Rank Chars by Physicochemical Properties. *Energy & Fuels, 27*, 7287−7293. http://dx.doi.org/10.1021/ef401639v

Jing, X. L., Wang, Z., Q., Yu, Z. L., Zhang, Q., Li, C. Y., & Fang, Y. T. (2013). Experimental and Kinetic Investigations of $CO_2$ Gasification of Fine Chars Separated from a Pilot-Scale Fluidized-Bed Gasifier. *Energy & Fuels, 27*, 2422-2430. http://dx.doi.org/10.1021/ef4002296

Kajitani, S., Hara, S., & Matsuda, H. (2002). Gasification rate analysis of coal char with a pressurized drop tube furnace. *Fuel, 81*(5), 539–546. http://dx.doi.org/10.1016/S0016-2361(01)00149-1

Kajitani, S., Zhang, Y., Umemoto, S., Ashizawa, M., & Hara. S. (2010). Co-gasification Reactivity of Coal and Woody Biomass in High-Temperature Gasification. *Energy & Fuels, 24*, 145-151. http://dx.doi.org/10.1021/ef900526h

Ke, Y. H., Yang, E. T., Liu, X., Liu, C. L., & Dong, W. S. (2013). Preparation of porous carbons from non-metallic fractions of waste printed circuit boards by chemical and physical activation. *New Carbon Materials, 28* (2), 108-114. http://dx.doi.org/10.1016/S1872-5805(13)60069-4

Kopyscinski, J., Habibi, R., Mims, C. A. & Hill, J. M. (2013). $K_2CO_3$-Catalyzed $CO_2$ Gasification of Ash-Free Coal: Kinetic Study. *Energy & Fuels, 27*, 4875−4883. http://dx.doi.org/10.1021/ef400552q

Lahijani, P., Zainal, Z. A., Mohamed, A. R., & Mohammadi, M. (2013). $CO_2$ gasification reactivity of biomass char: Catalytic influence of alkali,alkaline earth and transition metal salts. *Bioresource Technology, 144*, 288-295. http://dx.doi.org/10.1016/j.biortech.2013.06.059

Lahijania, P., Zainala, Z. A. & Mohamedb, A. R. (2012). Catalytic effect of iron species on $CO_2$ gasification reactivity of oil palm shell char. *Thermochimica Acta, 546*, 24-31. http://dx.doi.org/10.1016/j.tca.2012.07.023

Micco, G. D., Nasjleti, A., & Bohé, A. E. (2012). Kinetics of the gasification of a Rio Turbio coal under different pyrolysis temperatures. *Fuel, 95*, 537-543. http://dx.doi.org/10.1016/j.fuel.2011.12.057

Ochoal, J., Cassanello, M. C., Bonelli, P. R., & Cukierman, A. L. (2001). $CO_2$ gasification of Argentinean coal chars: a kinetic characterization. *Fuel Processing Technology, 74*, 161-176. http://dx.doi.org/10.1016/S0378-3820(01)00235-1

Ongondo, F. O., Williams, I. D., & Cherrett, T. J. (2011). How are WEEE doing? A global review of the

management of electrical and electronic wastes. *Waste Management, 31*, 714–730. http://dx.doi.10.1016/j.wasman.2010.10.023

Reif, A. E. (1952). The mechnism of the carbon dioxide-carbon reaction. *J. Phys. Chem., 56*, 785. http://dx.org/doi/abs/10.1021/j150498a033

Takarada, T., Tamai, Y., & Tomita, A. (1985). Reactivities of 34 coals under steam gasification. *Fule, 64*(10), 1438-1442. http://dx.doi.org/10.1016/0016-2361(85)90347-3.

Terakado, O., Ohhashi, R., & Hirasawa, M. (2011). Thermal degradation study of tetrabromobisphenol A under the presence metal oxide: Comparison of bromine fixation ability. *Journal of Analytical and Applied Pyrolysis, 91*, 303–309. http://dx.doi.10.1016/j.jaap.2011.03.006

United Nations Environment Programme [UNEP]. (2009). Retrieved from http://www.unep.org/yearbook/2009/

Yang, X. N., Sun, L. S., Xiang, J., Hu, H., & Su, S. (2013). Pyrolysis and dehalogenation of plastics from waste electrical and electronic equipment (WEEE): A review. *Waste Management, 33*, 462–473. http://dx.doi.org/10.1016/j.wasman.2012.07.025

Yuan, S., Chen, X. L., Li, J., & Wang, F. C. (2011). $CO_2$ Gasification Kinetics of Biomass Char Derived from High-Temperature Rapid Pyrolysis. *Energy & Fuels, 25*, 2314–2321. http://dx.doi.org/10.1021/ef200051z

Zhang, S. Z., Yoshikawa, K., Nakagome, H., & Kamo, T. (2013). Kinetics of the steam gasification of a phenolic circuit board in the presence of carbonates. *Applied Energy. 101*, 815–821. http://dx.doi.org/10.1016/j.apenergy.2012.08.030

Zhang, Y., Ashizawa, M., Kajitani, S., & Miura, K. (2008). Proposal of a semi-empirical kinetic model to reconcile with gasification reactivity profiles of biomass chars. *Fuel, 87*, 475-481. http://dx.doi.org/10.1016/j.fuel.2007.04.026

Zhang, Y., Hara, S., Kajitani, S., & Ashizawa, M. (2010). Modeling of catalytic gasification kinetics of coal char and carbon. *Fuel, 89*, 152-157. http://dx.doi.org/10.1016/j.fuel.2009.06.004